

Phase-field Modeling for Faceted Dendrite Growth of Silicon

Hisashi Kasajima, Toshio Suzuki*, Seong Gyoon Kim** and Won Tae Kim***

Graduate School, The University of Tokyo, Tokyo, 113-8656 Japan

Fax: 81-3-5841-8653, e-mail: kasa@mse.mm.t.u-tokyo.ac.jp

* Department of Materials Engineering, The University of Tokyo, Tokyo, 113-8656 Japan

Fax: 81-3-5841-8653, e-mail: suzuki@material.t.u-tokyo.ac.jp

** Department of Materials Science and Engineering, Kunsan National University, Kunsan, Korea

E-mail: sgkim@kunsan.ac.kr

*** Department of Physics, Chongju University, Chongju, Korea

E-mail: wontae@chongju.ac.kr

Faceted Dendrite growth was investigated by using a phase-field model for crystal growth with anisotropic interfacial energy. Phase-field parameters at the thin interface limit were derived and used in the simulation. The accuracy of the model was estimated from the calculated equilibrium interface shape. The errors in the anisotropy and Gibbs-Thomson effect were within 1% and 10%, respectively. The growth of a silicon crystal from its undercooled melt has been analyzed. The results show that a dendrite grows keeping its tip shape to be the same regardless of the growth velocity and that the tip size of a dendrite decreases with increase of the growth velocity.

Key words: phase-field model, faceted crystal, anisotropic interface energy, dendrite, silicon

1. INTRODUCTION

Recently many attentions have been paid to the dendrite growth of semiconductor materials from their undercooled melts, so as to obtain information on their crystal growth mechanism. Experiments have been carried out mainly for silicon and germanium and it is shown that the periphery surfaces of a dendrite are all (111) faces and the crystal growth behavior is classified into three categories: lateral growth, continuous growth and rapid growth at high undercooling [1-4]. The change of the growth mechanism has been investigated by the in-situ observation of growing interface morphology and the growth velocity at the ranges of lateral and continuous growth is shown to be approximately proportional to the square of the degree of undercooling [3,4]. Though the transition from lateral to continuous growth have been discussed using a conventional dendrite growth theory [4], the growth behavior of a silicon crystal is still not clear.

Phase-field modeling is one of the possible tools to analyze the growth of a faceted crystal. It is powerful in describing the growing interface morphology and a large number of examples show its wide applicability to the problems [5-8]. In addition it is shown that the thin interface limit phase-field model gives a quantitative prediction [9-11]. However, the model for the faceted crystal growth should be modified so as to include highly anisotropic interfacial energy as proposed by Egglestone et al. [12]. Namely the interface of a faceted crystal within a range of so-called missing orientations becomes unstable and the interface energy in the governing equation for missing orientations should be changed to that at the edge

of the stable orientation. Their model successfully reproduced the equilibrium shape and the growth of a faceted crystal.

In the present work the dendrite growth of silicon from its undercooled melt is investigated using a phase-field model with thin interface limit parameters. The morphology of a growing dendrite and its change with increase of growth velocity are examined and discussed.

2. CALCULATION

2.1. GOVERNING EQUATIONS

In two-dimensional phase-field modeling, the interface energy with four-fold symmetric anisotropy, $\sigma(\theta)$, is assumed as

$$\sigma(\theta) = \sigma_0(1 + \nu \cos 4\theta),$$

where ν is the intensity of anisotropy and θ is the angle between the direction normal to the interface and the x-axis. Here the orientation with the largest interface energy is taken to be the x-axis. The angle dependent curvature of radius, $R(\theta)$, is found from the Gibbs-Thomson equation.

$$(\sigma(\theta) + \sigma'(\theta))/R(\theta) = f^L - f^S,$$

where f^L and f^S are the free energy density of solid and liquid phases, respectively. Since the right hand side of the equation is positive in an isothermal system with a solid particle in a undercooled liquid, a convex non-faceted crystal becomes stable when $\nu < 1/15$. Conversely when $\nu > 1/15$, the left hand side of the equation becomes negative within the missing orientations. Then a faceted

crystal comes to be stable, which has the interface with stable orientations. The missing orientations correspond to the range with the concaved shape in the Wulff's plot. In order to get rid of the missing orientations, the anisotropic interfacial energy is modified as [12],

$$\sigma(\theta) = \frac{\sigma(\theta_m)}{\cos\theta_m} \cos\theta \quad (-\theta_m < \theta < \theta_m),$$

where θ_m is the first missing orientation and it is derived by

$$\frac{d}{d\theta} \left(\frac{\cos\theta}{\sigma(\theta)} \right) = 0.$$

The anisotropy of the interface kinetics is taken account in association with the anisotropy of the interface energy so as to have the same orientation dependence as the interface energy [10],

$$\beta(\theta) = 1/\mu(\theta) = \beta_0(1 - \nu_K \cos 4\theta)$$

where $\mu(\theta)$ and ν_K are the linear kinetic coefficient and its anisotropy, respectively.

A phase-field model for crystal growth is based on the Ginzburg-Landau free energy functional. The phase field, ϕ , is defined as 0 at liquid and 1 at solid and varies continuously from 0 to 1 within the interface region. The phase-field equations within stable orientations are given by

$$\begin{aligned} \frac{1}{M} \frac{\partial \phi}{\partial t} = & \varepsilon^2 \nabla^2 \phi \\ & + \varepsilon \varepsilon' \left\{ \sin 2\theta \cdot (\phi_{yy} - \phi_{xx}) + 2 \cos 2\theta \cdot \phi_{xy} \right\} \\ & - \frac{1}{2} (\varepsilon'^2 + \varepsilon \varepsilon'') \left\{ 2 \sin 2\theta \cdot \phi_{xy} - \nabla^2 \phi - \cos 2\theta \cdot (\phi_{yy} - \phi_{xx}) \right\} \\ & - f_\phi \end{aligned} \quad (1a)$$

and that within missing orientations is given by

$$\frac{1}{M} \frac{\partial \phi}{\partial t} = \left(\frac{\varepsilon(\theta_m)}{\cos\theta_m} \right)^2 \phi_{xx} - f_\phi \quad (1b)$$

where M , ε and W are phase-field parameters defined below, and the subscripts under ϕ and f denote the partial derivatives. Note that it guarantees the orientation continuity to take the average of the edge orientations at the adjacent points. The angle of the interface normal, the free energy density, f , the solid fraction, $h(\phi)$, and the parabolic potential, $g(\phi)$, are defined by

$$\tan \theta = \phi_y / \phi_x$$

$$f = h(\phi) f^s + (1 - h(\phi)) f^l + W g(\phi)$$

$$h(\phi) = \phi^2 (3 - 2\phi) \quad g(\phi) = \phi (1 - \phi).$$

The equation for thermal diffusion is given by

$$\frac{\partial T}{\partial t} = D \nabla^2 T + h'(\phi) \frac{\Delta H}{C_p} \frac{\partial \phi}{\partial t} \quad (2)$$

where D is the thermal diffusivity, ΔH is the latent heat per unit volume, and C_p is the specific heat per unit volume.

The phase-field parameters ε and W are related to the interface energy and the interface width, λ , respectively and M is related to the linear kinetic coefficient.

$$\lambda = \frac{4\sigma_0}{W} \quad \varepsilon = \frac{4\sqrt{2}}{\pi} \frac{\sigma_0}{\sqrt{W}}$$

$$M^{-1} = \frac{\varepsilon^2 \Delta H}{\sigma_0 T_m} \left[\frac{1}{\mu(\theta)} + \frac{\Delta H}{DC_p} \int_{-\infty}^{+\infty} \frac{h(\phi)(1-h(\phi))}{\sqrt{\phi(1-\phi)}} dx \right]$$

where T_m is the melting temperature. These parameters are derived at the thin interface limit.

2.2. NUMERICAL CALCULATION

For the numerical calculation Eqs.(1a), (1b) and (2) were discretized on uniform grids using an explicit finite difference scheme. In order to reduce the calculation time, the calculation area was divided into several areas with different mesh sizes. The time change of the phase-field was calculated in the area with the mesh size of Δx and the thermal field was calculated in the areas with the mesh size of 3, 9, 27, 81 and 243 Δx . During the calculation the areas were rearranged according to the interface movement so as to pursue the interface. The total length of the calculation area was at most 30000 Δx and the numerical calculation was carried out at the one-eighth space. The interface width, λ , was set to be 7 Δx . In the calculation all variables were rewritten into the dimensionless forms by using the following units of the capillary length, $d_0 = \sigma_0 T_m C_p / \Delta H^2$, the time, d_0^2 / D , and the temperature, $\Delta H / C_p$. The physical properties of silicon used in the calculation are shown in Table I. Note that the value of the linear kinetic coefficient was set to be larger than a usual value for the computational efficiency.

Table I Physical properties of silicon

Specific heat per volume, C_p	J/m ³ K	2.14 x 10 ⁶
Thermal diffusivity, D	m ² /s	2.80 x 10 ⁻⁵
Melting temperature, T_m	K	1685
Latent heat of fusion, ΔH	J/m ³	4.15 x 10 ⁹
Interface energy, σ_0	J/m ²	0.438
Anisotropy of interface energy, ν	-	0.15
Kinetic anisotropy, ν_K	-	0, 0.07, 0.13
Linear kinetic coefficient, μ	m/Ks	1.6

3. RESULTS AND DISCUSSIONS

Before the dendrite growth simulation the calculation accuracy by the model has been examined by comparing the calculated crystal shapes with the analytical equilibrium

ones. The anisotropy evaluated from the ratio of the maximum to minimum radius and the curvature radius at the position with the minimum interface energy are compared with analytical ones for different values of the dimensionless interface width, λ/d_0 . The errors in anisotropy and Gibbs-Thomson effect are within about 1% and 10%, respectively as shown in Table II.

Table II Errors in anisotropy and Gibbs-Thomson effect. (dimensionless undercooling, $\Delta \approx 0.025$).

error (%)	λ/d_0				
	2	5	10	20	50
Δv	0.56	0.39	0.99	1.09	0.65
$\Delta \sigma$	-6.27	-7.94	-7.53	-7.69	-7.64

Figure 1 shows a typical dendrite calculated under the condition of $\Delta=0.5$ and $\lambda/d_0=50$. The tip keeps its shape during the growth and the interface behind the tip becomes unstable to form secondary arms at the sides.



Fig.1 Typical dendrite shape ($\Delta=0.5$, $\lambda/d_0=50$).

To obtain the steady state growth of a dendrite the growth distance of the dendrite should be larger than its diffusion length. In addition the steady state growth velocity changes with the dimensionless interface width [9]. The capillary length of silicon is small so that it is difficult to attain the steady state when λ/d_0 is small and the steady state growth velocity was attained only for $\lambda/d_0 = 50$. Therefore the change in growth velocity with λ/d_0 is estimated by comparing the growth velocity for larger λ/d_0 with that for smaller one at the time when the later calculation was terminated (about 300 hours). Table III shows the relationship between the dimensionless growth velocity, $\tilde{v} = V/(D/d_0)$, and λ/d_0 . The growth velocity for $\lambda/d_0 = 50$ is about 20% smaller than that for $\lambda/d_0 = 2.5$. The growth velocity changes also with the kinetic anisotropy as shown in Table IV. The kinetic anisotropy does not affect the growth velocity much so that the calculation has been carried out without the kinetic anisotropy.

Table III Dimensionless Growth velocities, \tilde{v} , for different values of interface width. The growth velocities are compared at the same dimensionless time, $\tilde{t} (= t / (d_0^2/D))$ ($\Delta=0.5$).

$\tilde{v} \times 10^{-3}$	λ/d_0				
	2.5	5	10	20	50
734700	1.480	1.481			
2204000		1.307	1.236		
7347000			1.163	1.122	1.018

Table V Change in growth velocity with kinetic anisotropy. ($\Delta=0.5$, $\lambda/d_0=10$)

v_K	0	0.07	0.13
$\tilde{v} \times 10^{-3}$	1.165	1.136	1.098

In order to examine the dendrite tip shape and size in detail the calculation was carried out for $\lambda/d_0=50$, $v_K=0$ and $\Delta=0.05 \sim 0.6$. In the growth of a faceted dendrite its tip does not proceed continuously but conciliatorily. It is due to that the growth direction at the edge is given as the average values of adjacent points in the model and the adjacent interface grows preferably to the edge. During the growth the tip shape is kept to be the same and its size changes with growth velocity. In order to examine the growth velocity dependence on the tip shape and size, the dimensionless tip width, L_T , is evaluated as a function of the angle of the interface normal, θ , as shown in Fig.2.

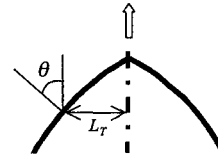


Fig.2 Schematic drawing of a faceted dendrite tip and the definitions of the tip width, L_T , and the angle of the interface normal, θ .

Figure 3 show the change in the normalized tip width with the angle of the interface normal calculated for different values of undercooling. In the figure the tip width is normalized by the value of L_T at $\theta = \pi/4$. Though the tip shape is different from the equilibrium one, it is the same regardless of growth velocity.

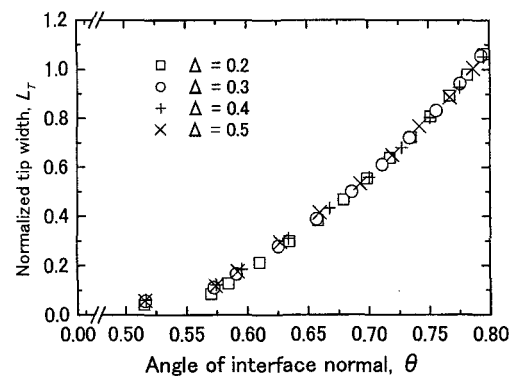


Fig.3 Normalized tip width ($=L_T(\theta)/L_T(\pi/4)$) vs. angle of interface normal ($\lambda/d_0=50$).

For a non-faceted dendrite it is known that there exists a scaling between the tip radius and the growth velocity. Figure 3 shows that the similar relationship is expected for a faceted dendrite growth when the tip width is taken as a characteristic length of the tip.

Figure 4 shows the relationship between the dimensionless tip width and the dimensionless growth velocity, which are plotted in logarithmic scales. As seen in the figure the tip width linearly decreases and then increases with increase of the growth velocity. The data are on a line in the range of the growth velocity less than 10^{-4} and the exponent of the growth velocity is -0.38 . Since the tip width is chosen arbitrarily as a characteristic length of the tip we may define it in a modified way. For example, when a certain length, L_0 , is subtracted from L_T , we obtain the scaling relationship, $(L_T - L_0)^2 \tilde{V} = \text{const.}$, where L_0 is about 1.3 times of the interface width. Therefore a scaling law presumably exists for a faceted dendrite though it needs the examination more in detail.

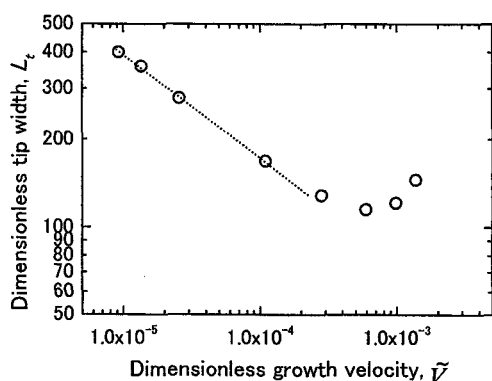


Fig.4 Dimensionless tip width vs. dimensionless growth velocity. The broken line is a guide to the eyes and demonstrates that the data are on a line.

4. CONCLUSIONS

The thin interface limit phase-field model has been successfully applied to the growth of a faceted crystal. The equilibrium shape of the crystal has been reproduced with good accuracy by the model. The errors of the anisotropy and the Gibbs-Thomson effect are within 1% and 10%, respectively. The growth of a silicon crystal from its

undercooled melt has been analyzed using the model. The results show that the tip shape of a faceted dendrite is the same regardless of the growth velocity and its size is presumably scaled to the growth velocity in a similar manner to a non-faceted dendrite.

ACKNOWLEDGEMENT

This work is partially supported by the Grant-in-Aid for Scientific Research (A) (No. 14205106) from the Ministry of Education, Culture, Sports, Science and Technology, Japan.

REFERENCES

- [1] C. F. Lau, H. W. Kui, *Acta Metall. Mater.*, **42**, 3811-16(1994)
- [2] D. Li, K. Eckler, D. M. Herlach, *Acta Mater.* **44**, 2437-43 (1996)
- [3] T. Aoyama, K. Kuribayashi, *Acta Mater.* **48**, 3739-3744 (2000)
- [4] T. Aoyama, K. Kuribayashi, *Mater. Sci. Eng. A*, **304**, 231-34 (2001)
- [5] M. Ode, T. Suzuki, S. G. Kim and W. T. Kim, *Sci. Tech. Adv. Mater.* **1**, 43-49 (2000)
- [6] W. J. Boettinger, S. R. Coriell, A. L. Greer, A. Karma, W. Kurz, M. Rappaz, R. Trivedi, *Acta Mater.* **48**, 43-70 (2000)
- [7] L. Q. Chen, *Ann. Rev. Mater. Res.* **32**, 113-140 (2002)
- [8] M. Ode, S. G. Kim, T. Suzuki, *ISIJ Int.* **41**, 1076-82 (2001)
- [9] A. Karma, W. J. Rappel, *Phys. Rev. E*, **57**, 4323-49 (1998)
- [10] J. Bragard, A. Karma, Y. H. Lee, M. Plapp, *Int. Sci.* **10**, 121-36 (2002)
- [11] S. G. Kim, W. T. Kim, T. Suzuki, *Phys. Rev. E*, **60**, 7186-97 (1999)
- [12] J. J. Eggleston, G. B. McFadden, P. W. Voorhees, *Physica D*, **150**, 91-103 (2001)

(Received October 13, 2003; Accepted March 17, 2004)